Controlling the Rashba spin-orbit interaction in quantum wells by adding a symmetric potential

Yoshiyuki Egami and Hiroshi Akera

Division of Applied Physics, Faculty of Engineering, Hokkaido University, Sapporo 060-8628, Japan

Incorporating a symmetric electrostatic potential into quantum wells (QWs) is proposed as a method to modify the coefficient α of the Rashba spin-orbit interaction. In a symmetric QW for which $\alpha = a_{\rm so}E_z$ with E_z the perpendicular electric field, the constant $a_{\rm so}$ can be controlled by the symmetric potential. The sign reversal of $a_{\rm so}$ with increasing the strength of the symmetric potential is demonstrated in (001)-oriented GaAs/AlGaAs QWs by a tight-binding model. The present findings can be used to realize structures with vanishing α in nonzero E_z.

The Rashba spin-orbit interaction (SOI)[1–4] is the origin of the intrinsic spin Hall effect predicted in a two-dimensional electron system (2DES),[5] and plays a key role in the action of many spintronic devices.[6] It has been experimentally shown in quantum wells (QWs) that the Rashba SOI can be controlled by the perpendicular electric field.[7–9] The rate at which the Rashba SOI changes with the electric field is determined by materials constituting each QW.[10] Therefore modifying the rate through material parameters is also effective in controlling the Rashba SOI. To be more precise, the Rashba SOI is written as, for an electron with in-plane wave vector (k_x, k_y) in the ground subband of the conduction band of a QW,

$$\hat{H}_{\rm so}^{\rm R} = \alpha(\sigma_x k_y - \sigma_y k_x), \tag{1}$$

where σ_x and σ_y are the Pauli spin matrices. In a QW with the structural inversion symmetry, the Rashba SOI is induced by the perpendicular electric field E_z and α is given by $\alpha = a_{\rm so}E_z$ at small enough E_z. The proportionality constant $a_{\rm so}$ depends on materials. In this paper we explore controlling the Rashba SOI through $a_{\rm so}$.

Controlling α by $a_{\rm so}$ is, in some cases, more convenient than by E_z. Reversing the sign of α is employed in various spintronic devices proposed recently, such as a triple-barrier spin filter consisting of two parallel 2DESs (formed by two QWs) with different signs of α[11] [Fig. 1(a)]. Such proposals considered producing positive and negative α by changing the direction of E_z. However, it is also possible to reverse the sign of α by changing the sign of $a_{\rm so}$. This

method has the advantage that it works in a uniform E_z (in a triple-barrier spin filter formed by two QWs with *different signs of* a_{so}, increasing the magnitude of uniform E_z gives the matching of spin-up levels in two QWs and that of spin-down levels in a sequential order, by making widths of two QWs different).

The vanishing of α is required in some phenomena and devices. The persistent spin helix, confirmed in recent experiments,[12–15] has been originally predicted[16] to occur in the case of $\alpha = 0$ in (110)-oriented QWs in addition to the case of $\alpha = \beta$ in (001)-oriented QWs, where β is the coupling constant of the Dresselhaus SOI[17] in the 2DES. The spin-lifetime field-effect transistor proposed recently[18] operates by switching α on and off. This proposal switches α by varying the electric field E_z from a large value to zero. However, it will be more flexible in application if α vanishes *even in the presence of* E_z by realizing $a_{so} = 0$. For example, consider two parallel 2DESs with $a_{so} = 0$ in one 2DES and $a_{so} \neq 0$ in the other [Fig. 1(b)], which are formed in a double QW. In this structure we can switch α on and off by moving electrons from one 2DES to the other *by the action of* E_z in which E_z changes the relative position of energy levels in two QWs. Such a device has the advantage that it does not require a fine tuning of E_z, while a precise tuning is necessary when we switch α off by setting E_z to zero.[19]

Reversing the sign of a_{so} can be implemented by varying band offsets between well and barrier layers in a QW structure as has been theoretically shown in our previous paper.[20] However the sign reversal of a_{so} with band offsets has a restriction in materials forming QWs: most QWs including a typical GaAs/AlGaAs QW have the type-I alignment giving only positive values of a_{so}.

In this paper we propose another method for the sign reversal of a_{so}, which combines a symmetric electrostatic potential with the potential induced by band offsets. The band-offset-induced potential [Fig. 1(c)], which changes discontinuously at interfaces, has different values at the conduction-band minimum, the maximum of the heavy-hole plus light-hole bands, and that of the split-off band. The symmetric electrostatic potential [Fig. 1(c)], denoted by $U(z)$, is the same in all bands and symmetric with respect to the well center $z = 0$. We demonstrate, employing a tight-binding model in (001)-oriented GaAs/AlGaAs QWs, that a_{so} successfully converts its sign from positive to negative owing to the symmetric electrostatic potential when it is lower in the well as in Fig. 1(c). Generation of an electrostatic potential in heterostructures has been experimentally demonstrated by introducing a microscopic capacitor consisting of donor (Si) and acceptor (Be) doped thin layers in each side of a GaAs/AlGaAs interface, which produce a doping interface dipole.[21] It has been achieved by the δ-doping

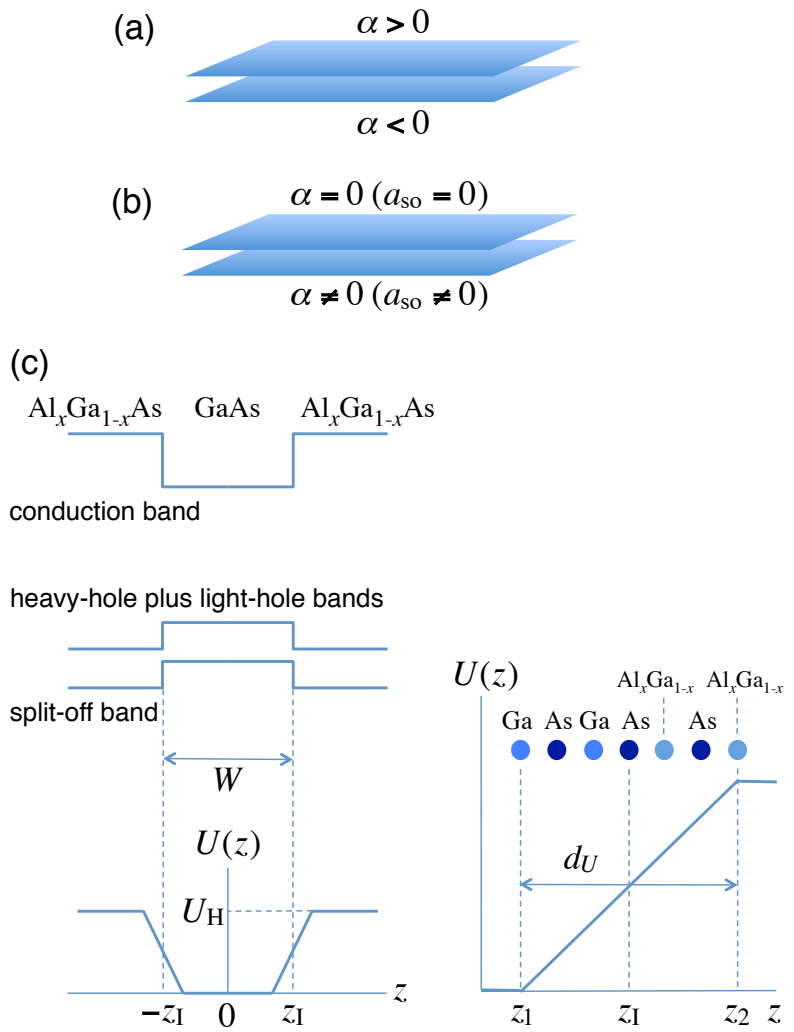

Fig. 1. (a) Two 2DESs with different signs of α because of different signs of a_{so}.
(b) One 2DES with $\alpha = 0$ ($a_{so} = 0$) and one with $\alpha \neq 0$ ($a_{so} \neq 0$) .
(c) Band-edge energies of the conduction band and the valence bands in a GaAs/AlGaAs quantum well, and a symmetric electrostatic potential $U(z)$.

method[22] that the width of doped layer reduces[23,24] to 10 Å and the doping areal density reaches[24] 10^{18} m^{-2} which produces the electric field of 10^9 V/m between two plates of the microscopic capacitor.

Our QW structure consists of GaAs in the well layer and $Al_xGa_{1-x}As$ in the barrier layer. The interfaces, placed on an As atomic layer, are parallel to the (001) plane of the zinc-blende structure. We apply the periodic boundary condition between sample boundaries placed in

the left and right barrier layers in calculating wave functions and energy levels. The barrier layer $(Al_xGa_{1-x}As)_{140}$ with width $70a = 396$ Å ($a = 5.65$Å is the lattice constant of GaAs since AlGaAs is lattice-matched to GaAs) is thick enough that the wave function decays to a negligible value at the boundaries.

We describe the symmetric electrostatic potential $U(z)$ by a model potential with in-plane translational symmetry. Our model potential is illustrated in Fig. 1(c) and given by $U(z) = 0$ $(0 < z < z_1)$, $U(z) = U_H(z - z_1)/(z_2 - z_1)$ $(z_1 < z < z_2)$, and $U(z) = U_H$ $(z_2 < z)$ with $U(-z) = U(z)$. The positions z_1 and z_2 are placed on Ga and Al_xGa_{1-x} atomic layers, respectively, which are at the same distance from the interface [the position of the interface becomes $z_I = (z_1 + z_2)/2$]. We denote the well width $2z_I$ by W and the thickness of the region with the variation of $U(z)$, $z_2 - z_1$, by d_U.

Actual systems with δ doping have two points which are not described by $U(z)$: (i) atomic energy levels in a donor (and similarly in an acceptor) are different from those of the host atom and (ii) the potential depends on x and y. However we focus on the effect of $U(z)$ on α because of the following reasons. With regard to the first point, we consider that the influence of the difference in atomic energy levels between donor and host atoms is small since the donor ionization energies of Si, Ge, and Sn in GaAs deviate only 4% from the effective Rydberg constant.[25,26] For the second point, the x and y dependence of the potential induces the level broadening $\hbar/\tau$ with τ the lifetime due to scatterings. However such scatterings depend on impurity distribution which we do not know precisely. In addition we expect that the ideal δ doping with a uniform impurity distribution can be realized in the future (a potential calculation for such ideal δ doping has already been performed[27]). For such reasons, many calculations on δ doping have been performed assuming the uniformity of potential along the xy plane.[22,28,29] According to these previous studies, we describe the potential by $U(z)$. In the following we explain limited information on the level broadening. (1) Quantum oscillations of the magnetoresistance, observed[28] in 2DESs formed by δ doping, have revealed a well-defined subband structure in agreement with the calculation assuming the in-plane translational symmetry, and suggested that the level broadening is less than a few meV. (2) In the lowest-order perturbation theory, the level broadening is determined by $\left|\left\langle k'_x k'_y \left| U_{\rm imp}(x,y,z) \right| k_x k_y \right\rangle\right|^2 \propto \left|\tilde{U}_{\rm imp}(q_x,q_y,z)\right|^2$ where $U_{\rm imp}(x,y,z)$ is the potential due to impurities, $\tilde{U}_{\rm imp}(q_x,q_y,z)$ is its two-dimensional Fourier transform, and (k_x,k_y) and (k'_x,k'_y) are wave vectors of initial and final states. The wavelength corresponding to (q_x,q_y) is larger than 10 nm for the small values of k_x,k_y and k'_x,k'_y considered in the present paper. Such long-wavelength component of the potential is suppressed by making the impurity distribution

uniform. Therefore the crystal-growth technique, which enhances the uniformity of impurity distribution, will reduce the level broadening.

The SOI acting on an electron in the ground subband of the conduction band in a (001)-oriented QW is expressed by the in-plane effective magnetic field, $B_x^{\rm eff}$ and $B_y^{\rm eff}$, as $\hat{H}_{\rm so} = B_x^{\rm eff}\sigma_x + B_y^{\rm eff}\sigma_y$ where the x and y axes are along [100] and [010] crystal axes, respectively. At small wave numbers k_x and k_y, $B_x^{\rm eff}$ and $B_y^{\rm eff}$ are expressed by the Rashba term (coefficient α) and the linear Dresselhaus term (β):

$$B_x^{\rm eff} = \alpha k_y + \beta k_x, \quad B_y^{\rm eff} = -\alpha k_x - \beta k_y. \tag{2}$$

The coefficients α and β can be obtained[30] from $B_x^{\rm eff}$ and $B_y^{\rm eff}$ at $(k_x, k_y) = (0, k)$ through $\alpha = B_x^{\rm eff}/k$ and $\beta = -B_y^{\rm eff}/k$, respectively. The components $B_x^{\rm eff}$ and $B_y^{\rm eff}$ are calculated[31] by $B_x^{\rm eff} = -\Delta_k \langle\sigma_x\rangle_k /2$ and $B_y^{\rm eff} = -\Delta_k \left\langle\sigma_y\right\rangle_k /2$, respectively, where Δ_k is the spin splitting between energy levels at $(k_x, k_y) = (0, k)$ in the ground subband of the conduction band and $\langle\sigma_x\rangle_k$ ($\left\langle\sigma_y\right\rangle_k$) is the expectation value of σ_x (σ_y) for the lower of the split levels.

We perform the sp^3s^* empirical tight-binding calculation[32] of energy levels and corresponding wave functions to obtain Δ_k and $\langle\sigma_x\rangle_k$. The wave function in the sp^3s^* tight-binding method is given by a linear combination of atomic orbitals, s, p_x, p_y, p_z, and s^* orbitals (s^* is an excited s state), in each of cation and anion atoms (Ga and As, respectively, in the case of GaAs) in well and barrier layers. Each orbital gives two bases corresponding to two spin states, for example, $|p_x\uparrow\rangle$ and $|p_x\downarrow\rangle$. Matrix elements of the Hamiltonian are obtained using tight-binding parameters, which are adjusted to reproduce the bulk band structure in each of well and barrier semiconductors. The spin-orbit interaction is taken into account by intra-atomic matrix elements between p-orbitals within each of cation and anion atoms and is expressed by tight-binding parameters, Δ_c and Δ_a, which are the spin-orbit splitting of p-levels in cation and anion atoms, respectively. The symmetric electrostatic potential $U(z)$ and the electric-field-induced potential, $eE_z z$ ($-e$ is the electron charge and $e > 0$), are taken into account in diagonal matrix elements.

We employ the tight-binding parameters presented in Ref. 33 for GaAs and AlAs and obtain parameters for $Al_xGa_{1-x}As$ from the linear interpolation between those of GaAs and AlAs, according to Ref. 33. These parameters accurately reproduce[33] the experimental values[34] of the conduction-band effective mass, the band gap and the valence-band spin-orbit splitting of GaAs, AlAs, and $Al_xGa_{1-x}As$ ($0 \le x \le 0.3$). We employ values obtained from Ref. 34 of the band offset in heavy-hole plus light-hole bands of $Al_xGa_{1-x}As$ relative to GaAs, $\Delta E_{\rm v}[{\rm eV}] = -0.53x$. We set intra-atomic tight-binding parameters of As atoms at each inter-

face equal to the average of those in GaAs and in $Al_xGa_{1-x}As$.

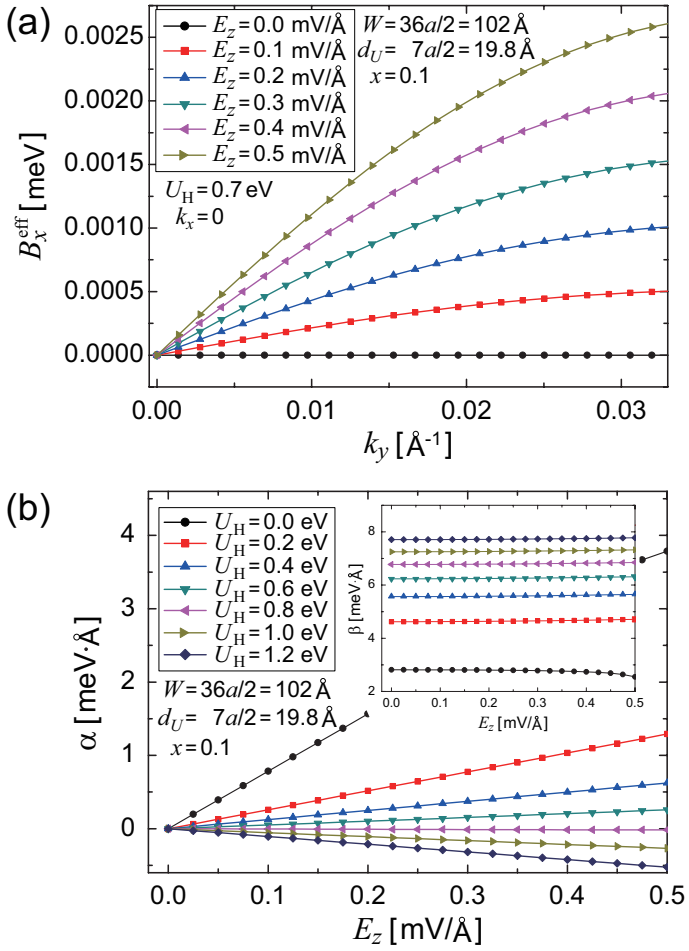

Fig. 2. Coefficient α of the Rashba SOI in a GaAs/$Al_xGa_{1-x}As$ QW with a symmetric electrostatic potential. (a) The x component of the effective magnetic field $B_x^{\rm eff}$ as a function of k_y at $k_x = 0$. (b) The E_z dependence of α calculated from $B_x^{\rm eff}$ at $k_y = 0.001(2\pi/a) = 0.001$ Å^{-1} through $\alpha = B_x^{\rm eff}/k_y$. The inset presents the E_z dependence of β, the coefficient of the Dresselhaus SOI, calculated from $B_y^{\rm eff}$ by $\beta = -B_y^{\rm eff}/k_y$.

Figure 2(a) presents calculated $B_x^{\rm eff}$ as a function of k_y at $k_x = 0$ for several values of E_z in a symmetric electrostatic potential with $U_{\rm H} = 0.7$ eV and $d_U = 7a/2 = 19.8$ Å in a GaAs/$Al_xGa_{1-x}As$ QW with $x = 0.1$ and the well layer consisting of $(GaAs)_{36}$ ($W = 36a/2 = 102$ Å). Each line shows that $B_x^{\rm eff}$ is linear in k_y when $k_y < 0.01(2\pi/a) = 0.01$ Å^{-1}. The slope of each line is α. Figure 2(b) presents α as a function of E_z for several values of $U_{\rm H}$ at a fixed value of $d_U = 19.8$ Å in the same QW, showing that α is linear in E_z at small values of E_z. Then we calculate the coefficient $a_{\rm so}$ by $a_{\rm so} = \alpha/E_z$. Figure 3(a) presents $a_{\rm so}$ as a function of $U_{\rm H}$ for several values of the Al fraction x. The value of $a_{\rm so}$ decreases with increasing $U_{\rm H}$ and with decreasing x. The sign of $a_{\rm so}$ is positive at $U_{\rm H} = 0$ ($x \geq 0.1$) and

converts to negative at $U_{\rm H} = 0.8$ eV for $x = 0.1$ and at a larger value of $U_{\rm H}$ with increasing x. Figure 3(b) and (c) show that, as we increase d_U or decrease W, $a_{\rm so}$ increases ($U_{\rm H} > 0.6$ eV), resulting in a shift of the $a_{\rm so}$-vanishing point to a larger $U_{\rm H}$.

The calculated coefficient of the Dresselhaus SOI, β, is also presented in Fig. 2(b) as a function of E_z for several values of $U_{\rm H}$, which shows that β depends only weakly on E_z and increases with increasing $U_{\rm H}$. Such dependences can be understood by the formula[35] $\beta = \gamma \left\langle \hat{k}_z^2 \right\rangle$ where γ is the Dresselhaus SOI constant of GaAs, $\left\langle \hat{k}_z^2 \right\rangle$ is the expectation value of $\hat{k}_z^2$ with respect to the ground-subband wave function, and $\hat{k}_z = -i\partial/\partial z$, since $\left\langle \hat{k}_z^2 \right\rangle$ has a weak dependence on E_z and increases as the confinement becomes stronger. The calculated value of $\beta = 8$ meV·Å at $U_{\rm H} = 1.2$ eV in Fig. 2(b) is close to the estimate of $\beta = \gamma \left\langle \hat{k}_z^2 \right\rangle = 7$ meV·Å which uses the sp^3s^* tight-binding value[36] of $\gamma = 10$ eV·Å^3 and the value of $\left\langle \hat{k}_z^2 \right\rangle$ from the present tight-binding calculation.

We discuss the above calculated results of α using the $\boldsymbol{k} \cdot \boldsymbol{p}$ approximation generalized to heterostructures.[10,37] Retaining terms to the lowest order in $kP/E_{\rm g}$, where k is the wave number, P is the Kane matrix element,[38] and $E_{\rm g}$ is the band gap, the coefficient α of the Rashba SOI in the ground subband of the conduction band is given by

$$\alpha = (P^2/3) \langle 0 | (\nabla_z G_{\rm v} - \nabla_z G_{\rm s}) | 0 \rangle , \tag{3}$$

where $\langle z|0\rangle = \varphi_0(z)$ is the ground-subband wave function and $\nabla_z = \partial/\partial z$. For the value of P we use that of the well material GaAs. Functions $G_{\rm v}(z)$ and $G_{\rm s}(z)$ are defined by $G_{\rm v}(z) = [E - E_{\rm v}(z) - V_{\rm es}(z)]^{-1}$ and $G_{\rm s}(z) = [E - E_{\rm s}(z) - V_{\rm es}(z)]^{-1}$ where the electron energy E is at the energy of the state $|0\rangle$ and $E_{\rm v}(z)$ [$E_{\rm s}(z)$] is the energy at the maximum of the heavy-hole plus light-hole bands [the split-off band]: $E_{\rm v}(z) = E_{\rm v}^{\rm W}$ [$E_{\rm s}(z) = E_{\rm s}^{\rm W}$] in the well layer and $E_{\rm v}(z) = E_{\rm v}^{\rm B}$ [$E_{\rm s}(z) = E_{\rm s}^{\rm B}$] in the barrier layer. The total electrostatic potential $V_{\rm es}(z)$ is given by $V_{\rm es}(z) = eE_z z + U(z)$. Then we have

$$\alpha = \left\langle 0 \left| \eta_{\rm es}(z)(eE_z + \nabla_z U) + \eta_{\rm bo}^{\rm v} \nabla_z E_{\rm v} - \eta_{\rm bo}^{\rm s} \nabla_z E_{\rm s} \right| 0 \right\rangle , \tag{4}$$

with

$$\eta_{\rm es} = \frac{P^2}{3}(G_{\rm v}^2 - G_{\rm s}^2),\ \eta_{\rm bo}^{\rm v} = \frac{P^2}{3} G_{\rm v}^{\rm W} G_{\rm v}^{\rm B},\ \eta_{\rm bo}^{\rm s} = \frac{P^2}{3} G_{\rm s}^{\rm W} G_{\rm s}^{\rm B}, \tag{5}$$

where $G_{\rm v}^{\rm W} = [E - E_{\rm v}^{\rm W} - U(z_{\rm I})]^{-1}$, $G_{\rm v}^{\rm B} = [E - E_{\rm v}^{\rm B} - U(z_{\rm I})]^{-1}$, and $G_{\rm s}^{\rm W}$ and $G_{\rm s}^{\rm B}$ are similarly defined. At small values of E_z, we have $\alpha = a_{\rm so} E_z$ with

$$a_{\rm so} = \int \left[e\eta_{\rm es}\rho_0 + \left(\eta_{\rm es}\nabla_z U + \eta_{\rm bo}^{\rm v} \nabla_z E_{\rm v} - \eta_{\rm bo}^{\rm s} \nabla_z E_{\rm s} \right) \frac{\rho_1}{E_z} \right] dz, \tag{6}$$

where $\rho_0 = [\rho(z) + \rho(-z)]/2 > 0$ and $\rho_1 = [\rho(z) - \rho(-z)]/2$ with $\rho(z) = |\varphi_0(z)|^2$. Here we

have neglected the E_z dependence of $\eta_{\rm es}$ and used that $U(z)$, $E_{\rm v}(z)$, and $E_{\rm s}(z)$ are symmetric with respect to the well center, $z = 0$. Equation (6) shows that $a_{\rm so} > 0$ when $U_{\rm H} = 0$ and that $a_{\rm so} < 0$ when $U_{\rm H}$ becomes large enough, since $\eta_{\rm es} > 0$, $\eta^{\rm v}_{\rm bo} > \eta^{\rm s}_{\rm bo} > 0$, $\rho_1/E_z < 0$ ($z > 0$), $\nabla_z U > 0$ ($z > 0$) in our model, and $\nabla_z E_{\rm v} \approx \nabla_z E_{\rm s} < 0$ ($z > 0$) in GaAs/AlGaAs QWs. With increasing the Al fraction x, the value of $|\nabla_z E_{\rm v}| \approx |\nabla_z E_{\rm s}|$ increases and then $a_{\rm so}$ increases. Such qualitative dependences on $U_{\rm H}$ and x of $a_{\rm so}$ are in agreement with the tight-binding calculation presented in Fig. 3(a). Quantitatively the $\boldsymbol{k} \cdot \boldsymbol{p}$ approximation to the lowest order in $kP/E_{\rm g}$ deviates from the tight-binding calculation at large values of $U_{\rm H}$, as demonstrated in Fig. 3(b).

The d_U dependence of $a_{\rm so}$ at larger values of $U_{\rm H}$ can be understood by considering the contribution to the integral $I_U = \int \eta_{\rm es}(\nabla_z U)(\rho_1/E_z)dz$ in Eq.(6) from the region $z_{\rm I} < z < z_2$ with a larger $\eta_{\rm es}$ [because of a larger $U(z)$]. As d_U decreases (the region with nonzero $\nabla_z U$ becomes thinner), the penetration of the wave function (and $|\rho_1(z)|$) into the region with larger $\eta_{\rm es}$ increases. This increased penetration leads to the increase of $|I_U|$ and then to a negative shift of $a_{\rm so}$ because $I_U < 0$. The W dependence, unfortunately, can not be explained by Eq.(6), since the correction to the present $\boldsymbol{k} \cdot \boldsymbol{p}$ approximation has a large W dependence.

In conclusion we have calculated the coefficient α of the Rashba SOI in (001)-oriented GaAs/AlGaAs QWs with a symmetric electrostatic potential by a tight-binding model, and found that the constant $a_{\rm so}$, which is defined by $\alpha = a_{\rm so}E_z$ with E_z the perpendicular electric field, changes its sign with increasing the strength of the symmetric potential. Therefore the symmetric electrostatic potential can be used to eliminate α in nonzero E_z.

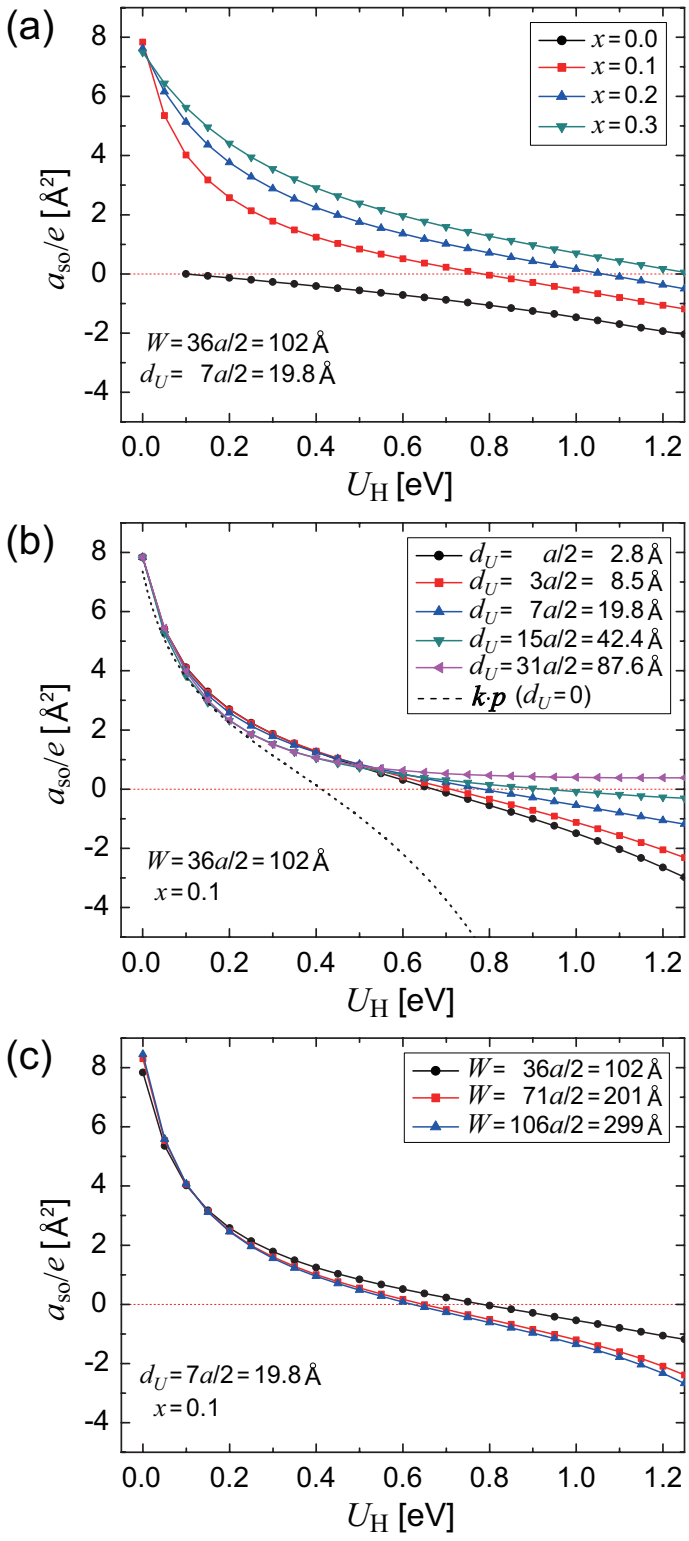

Fig. 3. Proportionality constant a_{so} (calculated from $a_{so} = \alpha/E_z$ at $E_z = 0.01$ mV/Å) of the Rashba SOI in a GaAs/Al$_x$Ga$_{1-x}$As QW with a symmetric electrostatic potential. (a) The x dependence of a_{so} as a function of U_H. (b) The d_U dependence of a_{so} as a function of U_H, with the $\boldsymbol{k}\cdot\boldsymbol{p}$ result corresponding to $d_U = 0$. (c) The well width W dependence of a_{so} as a function of U_H.

References

1) E. I. Rashba, Sov. Phys. Solid State **2**, 1109 (1960).
2) F. J. Ohkawa and Y. Uemura, J. Phys. Soc. Jpn. **37**, 1325 (1974).
3) Y. A. Bychkov and E. I. Rashba, J. Phys. C **17**, 6039 (1984).
4) Y. A. Bychkov and E. I. Rashba, JETP Lett. **39**, 78 (1984).
5) J. Sinova, D. Culcer, Q. Niu, N. A. Sinitsyn, T. Jungwirth, and A. H. MacDonald, Phys. Rev. Lett. **92**, 126603 (2004).
6) I. Žutić, J. Fabian, and S. D. Sarma, Rev. Mod. Phys. **76**, 323 (2004).
7) J. Nitta, T. Akazaki, H. Takayanagi, and T. Enoki, Phys. Rev. Lett. **78**, 1335 (1997).
8) G. Engels, J. Lange, T. Schäpers, and H. Lüth, Phys. Rev. B **55**, R1958 (1997).
9) T. Koga, J. Nitta, T. Akazaki, and H. Takayanagi, Phys. Rev. Lett. **89**, 046801 (2002).
10) R. Lassnig, Phys. Rev. B **31**, 8076 (1985).
11) T. Koga, J. Nitta, H. Takayanagi, and S. Datta, Phys. Rev. Lett. **88**, 126601 (2002).
12) J. D. Koralek, C. P. Weber, J. Orenstein, B. A. Bernevig, S.-C. Zhang, S. Mack, and D. D. Awschalom, Nature **458**, 610 (2009).
13) M. P. Walser, C. Reichl, W. Wegscheider, and G. Salis, Nat. Phys. **8**, 757 (2012).
14) M. Kohda, V. Lechner, Y. Kunihashi, T. Dollinger, P. Olbrich, C. Schönhuber, I. Caspers, V. V. Bel'kov, L. E. Golub, D. Weiss, K. Richter, J. Nitta, and S. D. Ganichev, Phys. Rev. B **86**, 081306 (2012).
15) J. Ishihara, Y. Ohno, and H. Ohno, Appl. Phys. Express **7**, 013001 (2014).
16) B. A. Bernevig, J. Orenstein, and S.-C. Zhang, Phys. Rev. Lett. **97**, 236601 (2006).
17) G. Dresselhaus, Phys. Rev. **100**, 580 (1955).
18) K. C. Hall, W. H. Lau, K. Gündoğdu, M. E. Flatté, and T. F. Boggess, Appl. Phys. Lett. **83**, 2937 (2003).
19) H. Akera, H. Suzuura, and Y. Egami, Phys. Rev. B **95**, 045301 (2017).
20) H. Akera, H. Suzuura, and Y. Egami, Phys. Rev. B **92**, 205311 (2015).
21) F. Capasso, A. Y. Cho, K. Mohammed, and P. W. Foy, Appl. Phys. Lett. **46**, 664 (1985).
22) K. Ploog, J. Cryst. Growth **81**, 304 (1987).
23) S. Modesti, D. Furlanetto, M. Piccin, S. Rubini, and A. Franciosi, Appl. Phys. Lett. **82**, 1932 (2003).
24) E. Carlino and V. Grillo, Phys. Rev. B **71**, 235303 (2005).
25) H. Fetterman, J. Waldman, C. Wolfe, G. Stillman, and C. Parker, Appl. Phys. Lett. **21**, 434 (1972).

26) M. Ozeki, K. Kitahara, K. Nakai, A. Shibatomi, K. Dazai, S. Okawa, and O. Ryuzan, Jpn. J. Appl. Phys. **16**, 1617 (1977).
27) A. Muñoz, N. Chetty, and R. M. Martin, Phys. Rev. B **41**, 2976 (1990).
28) A. Zrenner, F. Koch, and K. Ploog, Surf. Sci. **196**, 671 (1988).
29) J. J. Harris, J. Mater. Sci.: Mater. Electron. **4**, 93 (1993).
30) M. Murata and T. Tsuchiya, Physica E **42**, 2711 (2010).
31) M. O. Nestoklon, S. A. Tarasenko, J.-M. Jancu, and P. Voisin, Phys. Rev. B **85**, 205307 (2012).
32) P. Vogl, H. P. Hjalmarson, and J. D. Dow, J. Phys. Chem. Solids **44**, 365 (1983).
33) J. N. Schulman and Y.-C. Chang, Phys. Rev. B **31**, 2056 (1985).
34) I. Vurgaftman, J. R. Meyer, and L. R. Ram-Mohan, J. Appl. Phys. **89**, 5815 (2001).
35) M. I. Dyakonov and V. Y. Kachorovskii, Sov. Phys. Semicond. **20**, 110 (1986).
36) W. Knap, C. Skierbiszewski, A. Zduniak, E. Litwin-Staszewska, D. Bertho, F. Kobbi, J. L. Robert, G. E. Pikus, F. G. Pikus, S. V. Iordanskii, V. Mosser, K. Zekentes, and Yu. B. Lyanda-Geller, Phys. Rev. B **53**, 3912 (1996).
37) R. S. Calsaverini, E. Bernardes, J. C. Egues, and D. Loss, Phys. Rev. B **78**, 155313 (2008).
38) E. O. Kane, J. Phys. Chem. Solids **1**, 249 (1957).